JOURNAL OF THE AMERICAN CHEMICAL SOCIETY

Article

pubs.acs.org/JACS

Diels–Alder Reactivities of Strained and Unstrained Cycloalkenes with Normal and Inverse-Electron-Demand Dienes: Activation Barriers and Distortion/Interaction Analysis

Fang Liu,[†] Robert S. Paton,[‡] Seonah Kim,[†] Yong Liang,[†] and K. N. Houk*,[†]

[†]Department of Chemistry and Biochemistry, University of California, Los Angeles, California 90095, United States
[‡]Chemistry Research Laboratory, University of Oxford, Mansfield Road, Oxford OX1 3TA, United Kingdom

Supporting Information

ABSTRACT: The Diels–Alder reactions of the cycloalkenes, cyclohexene through cyclopropene, with a series of dienes—1,3-dimethoxybutadiene, cyclopentadiene, 3,6-dimethyltetrazine, and 3,6-bis(trifluoromethyl)-tetrazine—were studied with quantum mechanical calculations and compared with experimental values when available. The reactivities of cycloalkenes as dienophiles were found by a distortion/interaction analysis to be distortion controlled. The energies required for cycloalkenes to be distorted into the Diels–Alder transition states increase as the ring size of cycloalkenes increases from cyclopropene to cyclohexene, resulting in an increase in activation barriers. The reactivities of the dienes are controlled by both distortion and interaction energies. In normal Diels–Alder reactions with cycloalkenes, the electron-rich 1,3-dimethoxybutadiene exhibits stronger interaction energies than cyclopentadiene, but the high distortion energies required for 1,3-dimethoxybutadiene to achieve transition-state geometries overtake the favorable interaction, resulting in higher activation barriers. In inverse-electron-demand Diels–Alder reactions of 3,6-dimethyltetrazine and 3,6-bis(trifluoromethyl)tetrazine, the reactivities are mainly controlled by interaction energies.

INTRODUCTION

The high reactivity of cyclobutenone in the Diels–Alder reaction with cyclopentadiene was recently reported by Danishefsky and was analyzed by our group using the distortion/interaction model[1] (or activation strain model[2]). The reactivities of strained cycloalkenones were found to be a result of distortion acceleration. The distortion energies—the energies to distort the reactants into the transition-state geometries—correlated well with the activation energies.[3] By contrast, a poor correlation was observed between the activation energies and the reaction energies.

These trends in reactivity extend to cycloalkenes. Cyclopropenes are highly reactive dienophiles in Diels–Alder reactions even at low temperature[4] and have been applied in total synthesis[5] and bioorthogonal labeling.[6−8] Cyclobutenes and cyclopentenes are less reactive than cyclopropenes in Diels–Alder cycloadditions. The differences in the reactivities of cycloalkenes are apparent when one compares the cycloaddition reactions of cyclopropenes, cyclobutenes, and cyclopentenes with the same diene—cyclopentadiene (Scheme 1).[9−12]

The Diels–Alder reaction of cyclopropene with cyclopentadiene takes place at 0 °C (Scheme 1a), and a cyclopropene derivative reacts with cyclopentadiene at room temperature (Scheme 1b). Both reactions give excellent yields of adducts. The cycloaddition of a cyclobutene derivative with cyclopentadiene requires higher temperature of 80 °C, but still gives a good yield (Scheme 1c). The reaction of cyclopentene with cyclopentadiene requires heating to temperature as high as

Scheme 1. Reactions of Cyclopentadiene with Cycloalkenes in Diels–Alder Reactions

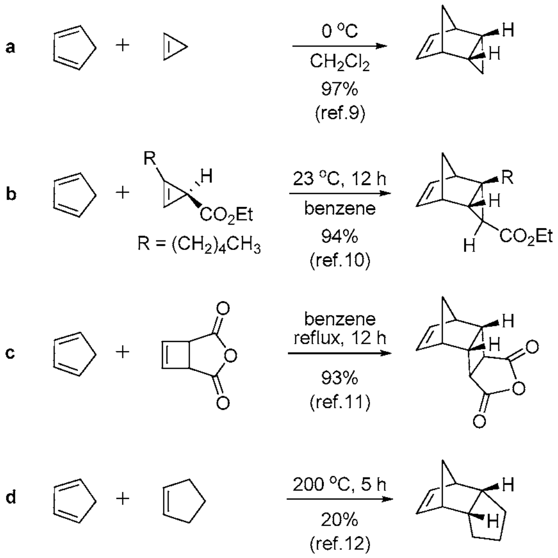

Received: August 14, 2013
Published: September 17, 2013

dx.doi.org/10.1021/ja408437u | J. Am. Chem. Soc. 2013, 135, 15642−15649

200 °C and gives a low yield (Scheme 1d). The Diels–Alder reactivities of cycloalkenes with cyclopentadiene increase from cyclopentene to cyclopropene. Similar trends of reactivity were found in the inverse-electron-demand Diels–Alder reactions of a 1,2,4,5-tetrazine with cycloalkenes, reported by Sauer et al. (Scheme 2).[13] The cycloaddition of cyclopropene and tetrazine is extremely fast, and an increase in the size of cycloalkenes by one roughly corresponds to a 100-fold decrease in the rate constant k_2.

Scheme 2. Reactivities of Cycloalkenes in Diels–Alder Reactions with 3,6-Bis(trifluoromethyl)tetrazine

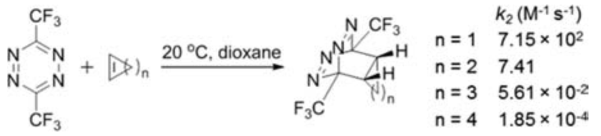

The high reactivity of three- and four-membered cycloalkenes has been attributed to strain-release, which is a thermodynamic factor, especially in ring-opening reactions.[14] However, the Diels–Alder reactions of cycloalkenes are different from ring-opening reactions in the sense that ring-strains are not fully released. If ring-strain accounts for the reactivity of cycloalkenes in Diels–Alder reactions, the difference between the strain energy of cycloalkenes (reactants) and the strain energy of the corresponding cycloalkanes that represents the strain energy of the cycloadduct should correlate with the rate constants shown in Scheme 2. Table 1 shows the strain energies (*SE*) of cycloalkenes and cycloalkanes obtained from the heat of combustion[15] and the strain energy differences (ΔSE).

Table 1. Strain Energies (*SE*, in kcal/mol) of Cycloalkenes and Cycloalkanes

	SE			ΔSE
cyclopropene	55.2	cyclopropane	27.5	**27.7**
cyclobutene	28.4	cyclobutane	26.5	**1.9**
cyclopentene	4.1	cyclopentane	6.2	**−2.1**
cyclohexene	−0.3	cyclohexane	0	**−0.3**

If strain-release were controlling reactivity, the orderly decrease in rate constants (k_2) from cyclopropene to cyclohexene should correspond to an orderly decrease in strain energy differences (ΔSE). However, the ΔSE values shown in Table 1 are erratic and really significant only for cyclopropene reactions. The Diels–Alder reaction of cyclopentene with 3,6-bis(trifluoromethyl)tetrazine is about 300 times faster than that of cyclohexene (Scheme 2), but strain energy changes would predict the opposite! Strain-release only influences the reactivity of cyclopropene and is not a general descriptor of reactivity. As we show later, cyclopropene is extraordinary in other ways as well.

Along the same line, the relationship between the heats of reaction and the activation enthalpies suggested by Brønsted, Marcus, and Bell–Evans–Polanyi were tested in previous studies of cycloaddition reactions. In general, these quantities correlate much less well with the activation barriers than distortion energies for cycloaddition reactions.[1,16,17]

Here we apply the distortion/interaction model to study the reactivities of cyclic alkenes including cyclopropene **5**, cyclobutene **6**, cyclopentene **7**, cyclohexene **8**, and acyclic alkene (*cis*-2-butene **9**) toward a series of dienes. Cyclopentadiene **1** and the electron-deficient 1,3-bis(trifluoromethyl)tetrazine **4** were selected in the study so that the computational results could be compared to experimental data. To investigate the electronic effect of dienes, the electron-rich 1,3-dimethoxybutadiene **2**, which is a simplified model for Danishefsky's diene **2′**,[18] and the less electron-deficient 3,6-dimethyltetrazine **3**, were also included in the study (Figure 1).

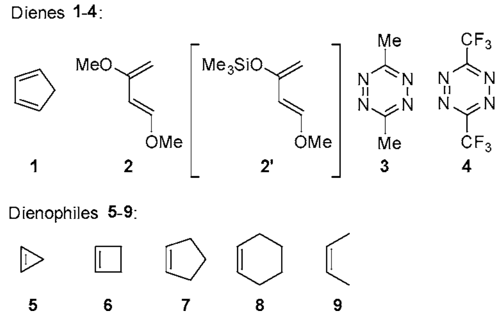

Figure 1. Dienes and dienophiles investigated.

■ COMPUTATIONAL METHODS

All density functional theory (DFT) calculations were performed with *Gaussian 09*.[19] Geometry optimization of all the minima and transition states involved was carried out at the M06-2X level of theory with the 6-31G(d) basis set,[20,21] which has been found to give relatively accurate energetics for cycloadditions.[22,23] The vibrational frequencies were computed at the same level to check whether each optimized structure is an energy minimum or a transition state and to evaluate its zero-point vibrational energy (ZPVE) and thermal corrections at 298 K. A quasiharmonic correction was applied during the entropy calculation by setting all positive frequencies that are less than 100 cm^{-1} to 100 cm^{-1}.[24,25] The frontier molecular orbitals (FMOs) and their energies were computed at the HF/6-311+G(d,p) level using the M06-2X/6-31G(d) geometries. Fragment distortion and interaction energies were computed at the M06-2X/6-31G(d) level. For the Diels–Alder reactions of 3,6-bis(trifluoromethyl)tetrazine, solvent effects in 1,4-dioxane, cyclohexane, dichloromethane, acetonitrile, and water were computed at the M06-2X/6-311+G(d,p) level using the gas-phase optimized structures. Solvation energies were evaluated by a self-consistent reaction field (SCRF) using the CPCM model,[26,27] where UFF radii were used. The scan of out-of-plane distortion dihedral angles of dienophiles **5**–**9** was performed by manually fixing the dihedral angles followed by an optimization at the M06-2X/6-31G(d) level. The formal atomic-hybridization states were obtained by a natural bond orbital (NBO)[28] analysis at the M06-2X/6-31G(d) level.

■ RESULTS AND DISCUSSION

The *endo* transition-state structures calculated at the M06-2X/6-31G(d) level for the Diels–Alder reactions between dienes **1** and dienophiles **5**–**9** are shown in Figure 2, left column. The *exo*-transition-state structures are provided in the Supporting Information (SI). The *endo* transition states are favored over the *exo* transition states by 1.8 to 4.3 kcal/mol in terms of free energy. The preference for *endo* transition states arises from favorable CH---π interactions in the *endo* structures[29] and unfavorable steric repulsion between methylene hydrogens on cyclopentadiene and alkenes in the *exo* structures.

The activation enthalpy ($\Delta H^{\ddagger}$), activation free energy ($\Delta G^{\ddagger}$), and free energy of reaction (ΔG_{rxn}) are shown below each structure in kcal/mol in blue, red, and black, respectively. The activation enthalpies and free energies of the Diels–Alder

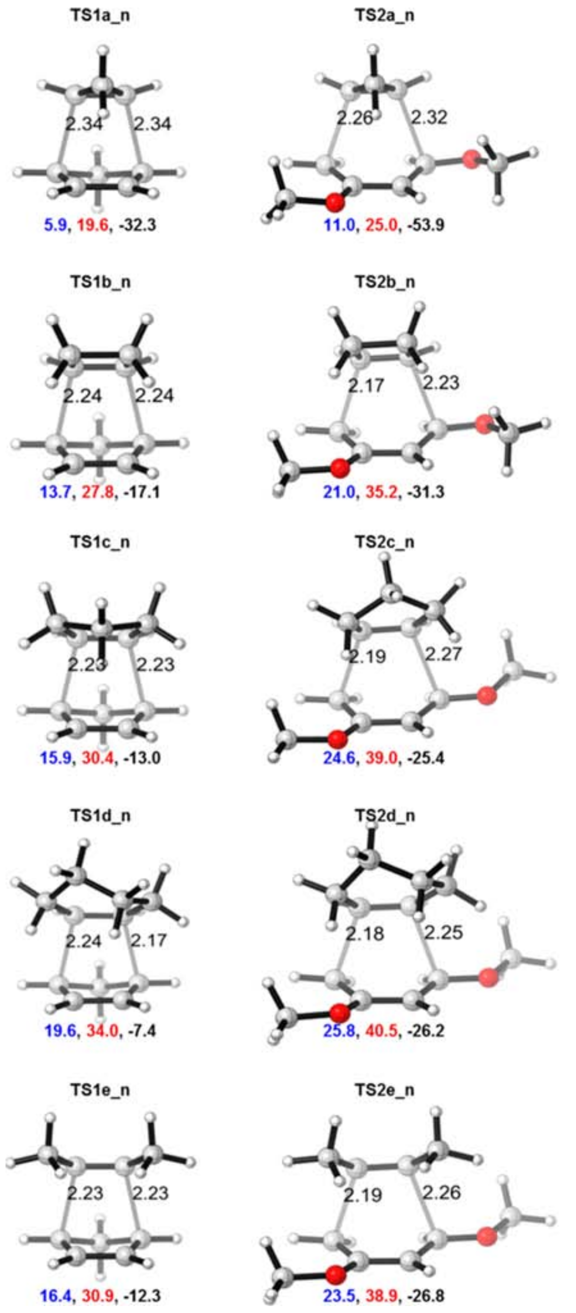

Figure 2. M06-2X/6-31G(d)-optimized *endo* transition structures for reactions of cyclopentadiene and 1,3-dimethoxybutadiene (forming C−C bonds are labeled in Å; $\Delta H^\ddagger$, $\Delta G^\ddagger$, and ΔG_{rxn} are shown below the structures in blue, red, and black, respectively, in kcal/mol).

reactions of cycloalkenes with cyclopentadiene increase from cyclopropene to cyclohexene, in agreement with the reported decrease in reactivities (Scheme 1). Cyclopropene readily undergoes Diels−Alder cycloaddition with cyclopentadiene at room temperature or below, which corresponds to a free energy barrier of about 20 kcal/mol. The reaction between cyclobutene derivative and cyclopentadiene must be performed in refluxing benzene (80 °C), in accord with the calculated higher barrier of 27.8 kcal/mol. The reaction of cyclopentene with cyclopentadiene requires even higher temperature of 200 °C, and accordingly the calculated barrier is larger, at 30.4 kcal/mol. Cyclohexene is calculated to be less reactive still than cyclopentene with a higher barrier (34.0 kcal/mol), and the reactivity of acyclic *cis*-2-butene falls in between cyclopentene and cyclohexene. The computed free energies of reaction increase from cyclopropene to cyclohexene, in accordance with the increase in activation energies.

The lengths of forming bonds are marked on transition-state structures in Å in Figure 2. Cyclohexene has an asynchronous transition state in which the forming bond distances differ by 0.07 Å resulting from the unsymmetrical structure of cyclohexene (Figure 2, **TS1d_n**). The other four dienophiles undergo synchronous cycloadditions with identical forming bond distances. Cyclopropene has an extremely early transition state (Figure 2, **TS1a_n**), consistent with the anomalously high exergonicity of this reaction ($\Delta G_{rxn} = -32.3$ kcal/mol), whereas the other ΔG_{rxn} values range from −7.4 to −17.1 kcal/mol. This change in transition-state position is in accordance with the Hammond's postulate. The forming bond distances are 0.1 Å larger than that observed in the transition state of cyclobutene with cyclopentadiene (Figure 2, **TS1b_n**). The transition states of cyclopentene and *cis*-2-butene fall between cyclobutene and cyclohexene. The trend of early-to-late transition state as measured by forming bond distance is: cyclopropene ≫ cyclobutene > cyclopentene ≈ *cis*-2-butene > cyclohexene, but only cyclopropene varies much from the others.

1,3-Dimethoxybutadiene (diene **2**) is a reasonable analogue to Danishefsky's diene, and has a similar free energy barrier in the Diels−Alder reaction with cyclobutene, as described in ref 18. The *endo* transition-state structures of the Diels−Alder reactions of diene **2** with dienophiles **5**−**9** are shown in Figure 2, right column (for each transition state, all possible conformations of the methoxy groups have been calculated, and the one with the lowest energy is shown here). The Diels−Alder reactions of 1,3-dimethoxybutadiene with alkenes **5**−**9** have asynchronous transition states compared to reactions of cyclopentadiene (Figure 2, **TS2a_n** through **TS2e_n**). C4 has the largest HOMO coefficient and most negative charge; therefore, it is the most nucleophilic carbon. In addition C4 is less hindered than C1, so the forming bond on C4 is 0.06−0.08 Å shorter than C1 in transition states. The *exo* transition-state structures are provided in the Supporting Information. The *endo* transition states are favored over the *exo* transition states by 0.4 to 1.7 kcal/mol. The preference for the *endo* transition states is less significant compared to that in the Diels−Alder reactions of cyclopentadiene, because there are less unfavorable steric repulsions in the *exo* transition states involving 1,3-dimethoxybutadiene. Similar trends of activation energies ($\Delta H^\ddagger$ and $\Delta G^\ddagger$) and reaction energies (ΔG_{rxn}) are found as in the reactions of dienes **2** and **1** with dienophiles **5**−**9**. The most significant difference between diene **1** and **2** is in terms of reactivity: 1,3-dimethoxybutadiene has a higher free energy barrier of 5.4−8.6 kcal/mol than cyclopentadiene in the cycloaddition to the same alkene. The electron-rich diene is 10^3−10^6 less reactive than cyclopentadiene, presumably due to the much larger distortion energy of the acyclic diene, as described in detail later. The trend of early/late transition states and reaction barriers with **2** are the same as those observed in the Diels−Alder reactions of alkenes with cyclopentadiene, **1**.

To understand this trend of Diels−Alder reactivity, each transition structure was separated into two fragments (the distorted dienophile and diene), followed by single-point energy calculations on each fragment. The energy differences between the distorted structures and optimized ground-state structures are the distortion energy of dienophile ($\Delta E^{\ddagger}_{dist\_2e}$)

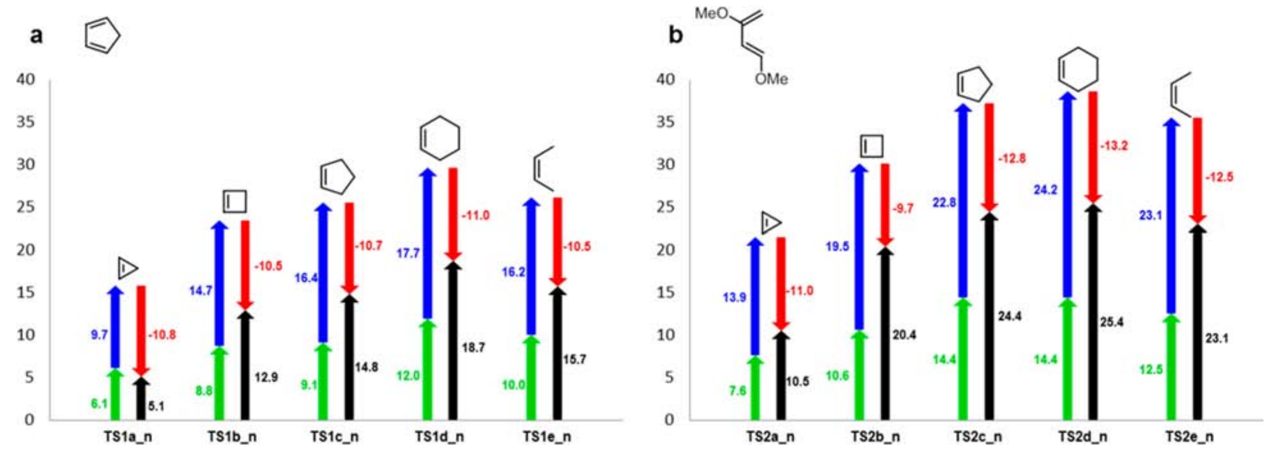

Figure 3. Graph of distortion, interaction, and activation energies for reactions of dienes **1** and **2** with dienophiles **5**−**9** (green: distortion energy of dienophile, blue: distortion energy of diene, red: interaction energy, black: activation energy, in kcal/mol).

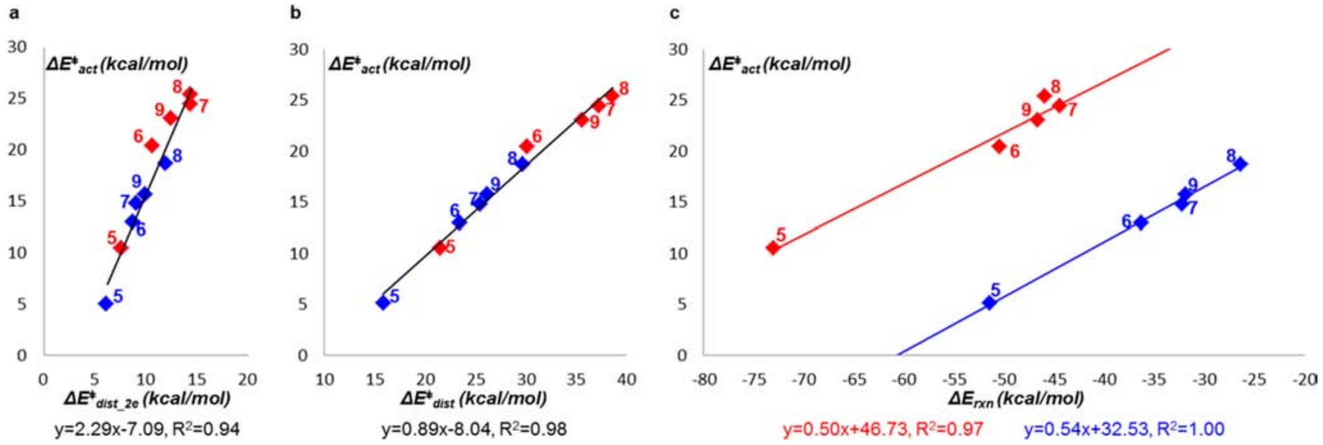

Figure 4. Plots of activation energy ($\Delta E^{\ddagger}_{\text{act}}$) vs (a) distortion energy of dienophile ($\Delta E^{\ddagger}_{\text{dist\_2e}}$), (b) total distortion energy ($\Delta E^{\ddagger}_{\text{dist}}$), and (c) reaction energy (ΔE_{rxn}). Blue: cyclopentadienes; red: 1,3-dimethoxybutadiene; black: overall correlation of all ten reactions (individual correlations for distortion energy and activation energy are not shown for clarity, see the SI). Linear correlation functions are shown below each plot in corresponding colors. The numbers shown besides each data point refer to the dienophiles involved in the corresponding reactions.

and diene ($\Delta E^{\ddagger}_{\text{dist\_4e}}$), respectively. The interaction energy ($\Delta E^{\ddagger}_{\text{int}}$) is the difference between the activation energy ($\Delta E^{\ddagger}_{\text{act}}$) and the total distortion energy ($\Delta E^{\ddagger}_{\text{dist}} = \Delta E^{\ddagger}_{\text{dist\_2e}} + \Delta E^{\ddagger}_{\text{dist\_4e}}$). The energy components for each *endo* transition-state structure are plotted in Figure 3 (see the SI for the analysis of the *exo* transition states).

Figure 3a shows the distortion/interaction analysis of the five Diels−Alder reactions with cyclopentadiene. The lengths of the green arrows represent the distortion energies of dienophiles ($\Delta E^{\ddagger}_{\text{dist\_2e}}$), which increase from 6 to 12 kcal/mol as the dienophile changes from cyclopropene to cyclohexene, while *cis*-2-butene falls in between cyclopentene and cyclohexene. The lengths of the blue arrows represent the distortion energies of cyclopentadienes ($\Delta E^{\ddagger}_{\text{dist\_4e}}$). There is an increase in $\Delta E^{\ddagger}_{\text{dist\_4e}}$ as the dienophile changes from cyclopropene to cyclohexene, consistent with the trend of early/late transition states. The geometry of early transition state is closer to the geometry of ground state, making the distortion energy smaller, and vice versa. The total length of blue and green arrows equals the total distortion energy ($\Delta E^{\ddagger}_{\text{dist}}$). The interaction energies ($\Delta E^{\ddagger}_{\text{int}}$) are represented by the red arrows pointing down starting from the values of total distortion energies. The interaction energies remain essentially constant across the series, ranging only from −11.0 to −10.5 kcal/mol. The distortion energies determine reactivities. Similar trends of distortion and activation energies are found in the distortion/interaction analysis of reactions of diene **2** in Figure 3b. A significant difference of Figure 3b from 3a is that 1,3-dimethoxybutadiene exhibits larger $\Delta E^{\ddagger}_{\text{dist\_4e}}$ than cyclopentadiene, resulting in larger reaction barriers. Details are discussed later herein.

Figure 4 shows the relationship between activation energy ($\Delta E^{\ddagger}_{\text{act}}$) and distortion energy ($\Delta E^{\ddagger}_{\text{dist\_2e}}$ and $\Delta E^{\ddagger}_{\text{dist}}$) and $\Delta E^{\ddagger}_{\text{act}}$ with the reaction energy (ΔE_{rxn}). The blue and red dots on the plot are for the Diels−Alder reactions of dienophiles **5**−**9** with diene **1** and **2**, respectively. For reactions of a given diene (Figure 4, either red or blue plot), both distortion energies and reaction energies correlate well with activation energies; R^2 values range from 0.92 to 1.00 (see the SI for individual correlation of distortion energy and activation energy). Taking the two sets of reactions together, the correlation between activation energy and reaction energy disappears ($R^2 = 0.16$). In particular, the Diels−Alder reactions of cyclopentadiene are over 10 kcal/mol less exothermic than those of 1,3-dimethoxybutadiene due to the less stable tricyclic adducts from the reactions, but the activation barriers are over 5 kcal/mol lower than those of the corresponding reactions of 1,3-dimethoxybutadiene. The correlation between distortion energy and activation energy is much better, with $R^2 = 0.94$ and 0.98, respectively (Figure 4, black lines).

Comparing a and b of Figure 3, the average interaction energy ($\Delta E^{\ddagger}_{\text{int}}$) in Figure 3b is 1.1 kcal/mol larger than in Figure 3a due to the smaller HOMO−LUMO gap involving diene **2** (see later discussion herein). However, the acyclic diene **2** exhibits large distortion energies due to the conformational change from *s-trans* to *s-cis* ($\Delta E = 2.2$ kcal/mol) and the steric repulsion of terminal hydrogen atoms in the transition states. Cyclopentadiene is predistorted toward the transition-state geometry and requires only bending and some bond-length changes. The average distortion energy of 1,3-dimethoxybutadiene is 5.8 kcal/mol higher than that of cyclopentadiene (Figure 3). The extra cost of distortion energies of 1,3-dimethoxybutadiene overtakes its advantage in interaction energies, resulting in a higher activation barrier of about 5 kcal/mol for each reaction compared with those of cyclopentadiene.

Figure 5 shows the transition-state structures calculated at the M06-2X/6-31G(d) level for the inverse-electron-demand Diels−Alder reactions between dienes **3** and **4** and dienophiles **5**−**9**. The activation enthalpy ($\Delta H^{\ddagger}$), activation free energy ($\Delta G^{\ddagger}$), and free energy of reaction (ΔG_{rxn}) are shown below each structure in kcal/mol in blue, red, and black, respectively. The lengths of forming bonds are marked on transition-state structures in Å. The reactions of both tetrazines and cyclopropene have very early transition states. Along the series of dienophiles changing from cyclopropene to cyclohexene, shorter forming bonds are observed. The more electrophilic tetrazine **4** has an earlier transition state than tetrazine **3** for each reaction. Each transition state on the right in Figure 5 has longer forming bonds of 0.1 Å and a lower free energy barrier of 10 kcal/mol than the corresponding transition state on the left. The activation free energies in the 1,4-dioxane solution $\Delta G^{\ddagger}_{\text{sol}}$ for reactions between diene **4** and dienophiles **5**−**8** have been calculated. The rate constants derived from calculated barriers by transition-state theory correlate well with the rate constants measured in experiments (Scheme 2), although theory consistently underestimates the barrier by 1−2 kcal/mol. The activation free energies in other solvents, including cyclohexane, dichloromethane, acetonitrile, and water, have been calculated as well (see the SI for details). The activation free energies in solution are higher than the gas phase results by 2−3 kcal/mol, because solvents stabilize tetrazine significantly.

The distortion/interaction analysis for the inverse-electron-demand Diels−Alder reactions is shown in Figure 6. Leaving out the reaction between cyclopropene and 3,6-dimethyltetrazine, which has an extremely early transition state, the interaction energies of the other four reactions fall in the small range of −21.6 to −18.0 kcal/mol (Figure 6a). The activation barriers increase along with the distortion energies from cyclobutene to cyclohexene. In other words, the reactivity differences of cycloalkenes in Diels−Alder reactions with 3,6-dimethyltetrazine originate from the distortion energy differences. Figure 6b shows the same trend of distortion and interaction energies. The activation barriers are much lower than Figure 6a due to stronger interaction energies, which result from smaller HOMO−LUMO gaps that are discussed later herein. Both the distortion energy and reaction energy correlate linearly with the activation energy for a single tetrazine (Figure 7), R^2 values range from 0.74 to 1.00. The correlation between the distortion energy and the activation energy has a slight advantage over that of the reaction energy.

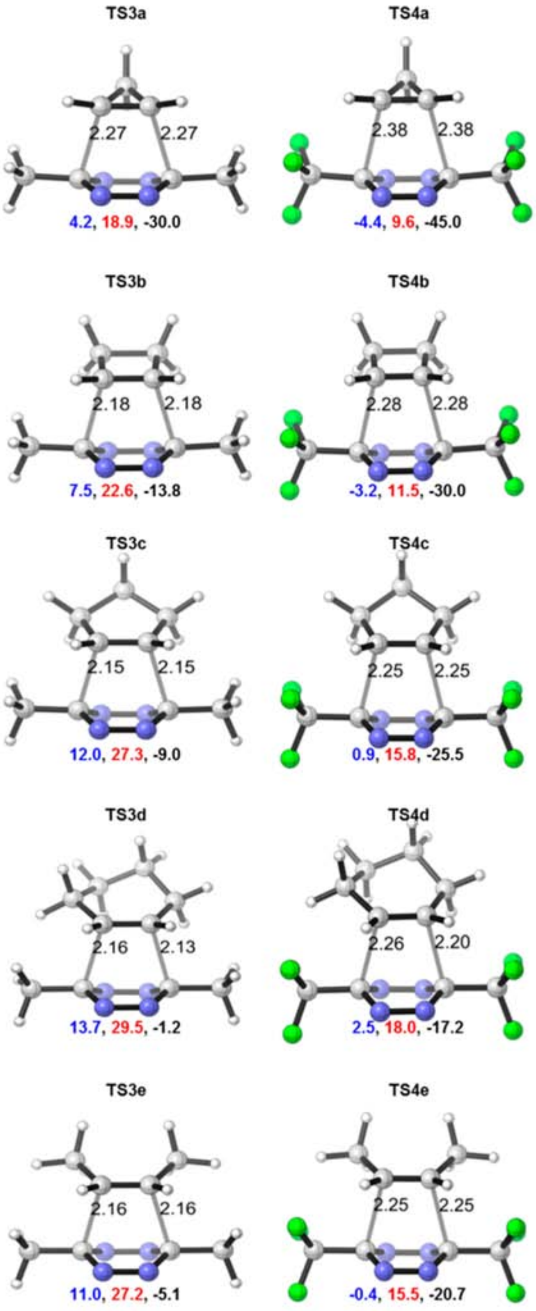

Figure 5. M06-2X/6-31G(d)-optimized transition structures for reactions of dienes **3** and **4** (forming C−C bonds are labeled in Å; $\Delta H^{\ddagger}$, $\Delta G^{\ddagger}$, and ΔG_{rxn} are shown below the structures in blue, red, and black, respectively, in kcal/mol).

Taking the two sets of reactions together, the correlations between distortion energies and activation energies are abolished due to the huge difference in interaction energies of diene **3** and **4**. The interaction energies of diene **4** are 3.9−7.6 kcal/mol stronger (more negative) than those of diene **3** in reactions with each dienophile, resulting in low-lying data points on the distortion/activation plot.

To better understand the interaction energy differences, the energies of relevant frontier orbitals were calculated at HF/6-311+G(d,p) level based on M06-2X/6-31G(d)-optimized reactants or transition-state geometries, because Kohn−Sham orbitals often provide poor estimates of ionization potentials of

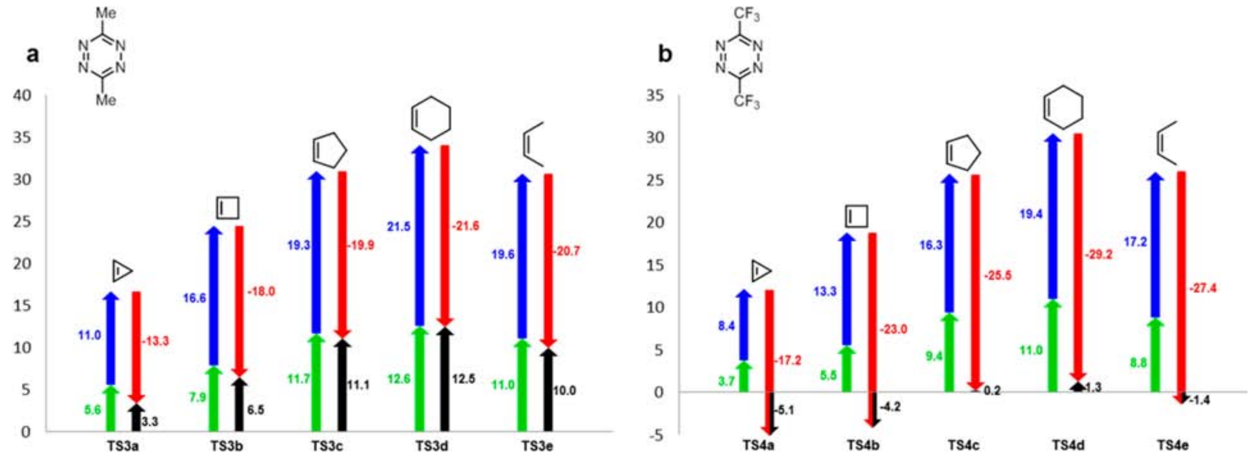

Figure 6. Graph of distortion, interaction, and activation energies for reactions of dienes **3** and **4** with dienophiles **5−9** (green: distortion energy of dienophile, blue: distortion energy of diene, red: interaction energy, black: activation energy, in kcal/mol).

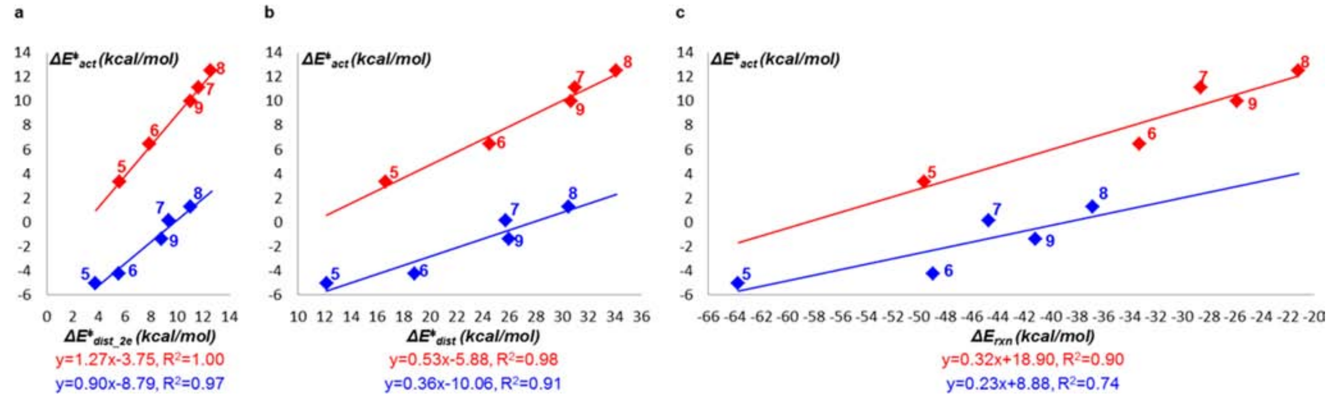

Figure 7. Plots of activation energy ($\Delta E^{\ddagger}_{\text{act}}$) vs (a) distortion energy of dienophile ($\Delta E^{\ddagger}_{\text{dist\_2e}}$), (b) total distortion energy ($\Delta E^{\ddagger}_{\text{dist}}$), and (c) reaction energy (ΔE_{rxn}). Blue: 3,6-bis(trifluoromethyl)tetrazine; red: 3,6-dimethyltetrazine. Linear correlation functions are shown below each plot in corresponding colors. The numbers shown besides each data point refer to the dienophiles involved in the corresponding reactions.

simple organic molecules and the medium size 6-31G(d) basis set often gives inaccurate unoccupied orbital eigenvalues.[30] As shown in Figure 8, the left column of each region shows the HOMOs and LUMOs of ground-state reactants, including the five alkenes and four dienes; the right column of each region shows the HOMOs and LUMOs of corresponding reactants distorted to the transition-state geometries of the reactions of dienes **1−4** and *cis*-2-butene, i.e. **TS1e_n**, **TS2e_n**, **TS3e**, and **TS4e**.

Calculations indicate that cycloalkenes have very similar HOMO and LUMO energies with the increase of ring size (Figure 8a). The HOMO energies range from −9.7 to −9.3 eV and the LUMO energies range from 2.9 to 4.0 eV. These data are close to experimental values measured from photoelectron spectroscopy (cyclopropene, −9.86 eV; cyclobutene, −9.59 eV; cyclopentene, −9.18 eV; cyclohexene, −8.94 eV)[31] and the electron affinities established from electron transmission spectroscopy (cyclopropene, 1.73 eV; cyclobutene, 2.00 eV; cyclopentene, 2.14 eV; cyclohexene, 2.13 eV).[32] The HOMO and LUMO energies of varies dienes decrease from the most electron-rich 1,3-dimethoxybutadiene to the most electron-deficient 3,6-bis(trifluoromethyl)tetrazine (Figure 8b−e). In normal Diels−Alder reactions, the HOMO of diene interacts with the LUMO of the dienophile and smaller HOMO−LUMO gap gives better interaction. Since the HOMO of 1,3-dimethoxybutadiene is 0.2 eV higher than cyclopentadiene

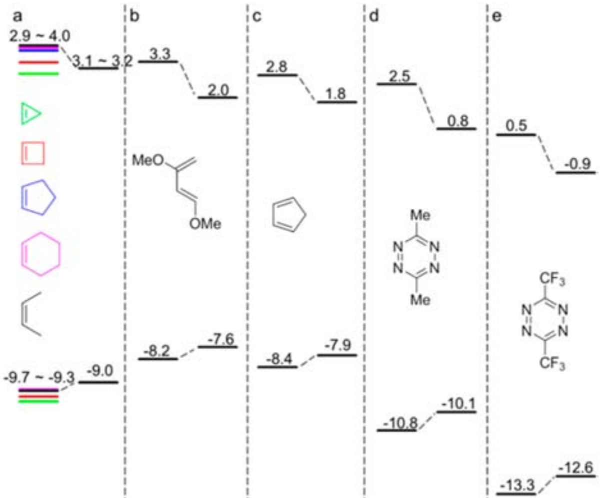

Figure 8. FMO energies for (a) alkenes (cyclopropene, cyclobutene, cyclopentene, cyclohexene, and *cis*-2-butene) and (b−e) dienes (1,3-dimethoxybutadiene, cyclopentadienes, 3,6-dimethyltetrazine, and 3,6-bis(trifluoromethyl)tetrazine). HF/6-311+G(d,p)//M06-2X/6-31G(d)-computed orbital energies are shown in eV. The dashed lines indicate the change from ground-state reactant (left in each column) to distorted geometry in transition state (right in each column).

(Figure 9), it is expected that the interaction energies in Diels–Alder reactions of 1,3-dimethoxybutadiene are stronger than cyclopentadiene as discussed in Figure 3. In inverse-electron-demand Diels–Alder reactions, which involve the interaction between HOMOs of dienophiles and the LUMOs of dienes, the more electron-deficient 3,6-bis(trifluoromethyl)tetrazine has stronger interaction energies because the interacting unoccupied orbital is 2.0 eV lower than that of 3,6-dimethyltetrazine (Figure 9).

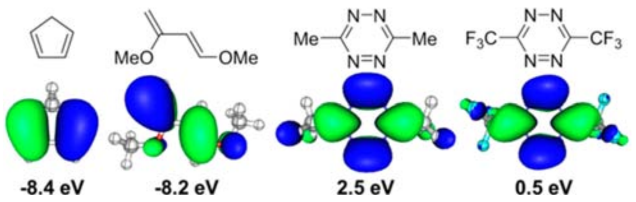

Figure 9. Important frontier molecular orbitals involved in the Diels–Alder reactions of dienes **1**–**4**: the HOMOs of cyclopentadiene and 1,3-dimethoxybutadiene and the low-lying vacant orbitals of 3,6-dimethyltetrazine and 3,6-bis(trifluoromethyl)tetrazine.

As the reactants are distorted into transition-state geometries, a decrease in LUMO energy by about 1 eV and an increase in HOMO energy by about 0.5 eV are observed (right columns of Figure 8a-e). The HOMO–LUMO gap shrinks by about 1.5 eV compared to that in ground-state reactants. The distortion of reactants facilitates the interaction between molecular orbitals of interest, namely the π and π* orbitals.

The Diels–Alder relative reactivities of different alkenes originate from the distortion energies. The trends of distortion energies are confirmed by a scan of out-of-plane distortion, which is a prominent distortion in the transition state (Figure 10). For each alkene, the out-of-plane dihedral angles, which are around 180° for ground-state structure and 140°–155° for transition-state structure, were gradually changed from 175° to 140° at intervals of 5°. The energy difference between optimized structure with fixed dihedral angles and the ground-state structure is called distortion energy of the dihedral angle ($\Delta E_{\text{dist\_}\varphi}$). Figure 10 shows the plot of $\Delta E_{\text{dist\_}\varphi}$ vs the dihedral angle φ.

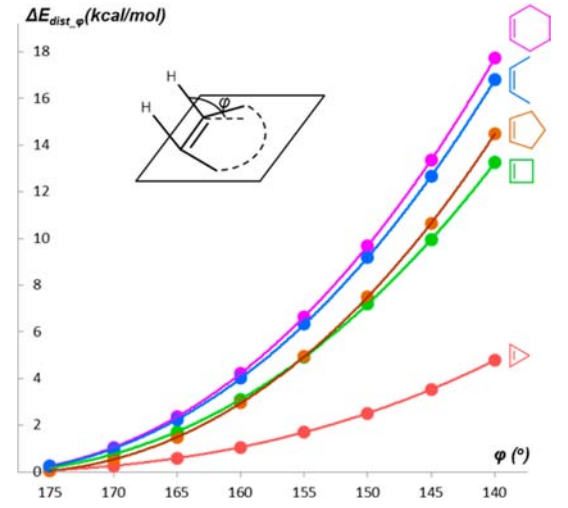

Figure 10. Plot of distortion energy ($\Delta E_{\text{dist\_}\varphi}$) vs out-of-plane distortion angle (φ) for dienophiles **5**–**9**. Red: cyclopropene; green: cyclobutene; brown: cyclopentene; purple: cyclohexene; blue: *cis*-2-butene.

For each alkene, the distortion energy increases as the dihedral angle decreases. At a certain dihedral angle within the transition zone (φ = 140–155°), the distortion energy of cyclopropene is significantly lower than other dienophiles, and as size increases from cyclopropene to cyclohexene, the distortion energy increases. This trend is consistent with the Diels–Alder reactivities of different alkenes discussed in this contribution. The increase in distortion energy of dihedral angles indicates an increase of out-of-plane bending force constants from cyclopropene to cyclohexene, which is confirmed by the C–H out-of-plane vibration frequency observed in IR spectra of cycloalkenes (γ-CH out-of-plane bend of cycloalkenes **5**–**8** are 570,[33] 635,[34] 695,[35] and 718 cm^{-1},[36] respectively). This trend in bending force constants is in accord with the change of hybridization states of the olefinic carbons suggested by the natural bond orbital (NBO) analysis. The corresponding hybridization states in cycloalkenes **5**–**8** (cyclopropene to cyclohexene) are $sp^{1.54}$, $sp^{1.92}$, $sp^{2.17}$, and $sp^{2.43}$, respectively.

■ CONCLUSION

The reactivities of cycloalkenes as dienophiles are controlled by distortion energies. Cyclopropene is more reactive than other alkenes because of the low distortion energy to achieve transition-state geometry. A larger degree of s character of the olefinic carbon results in relatively less sensitivity to out-of-plane bending, leading to a smaller force constant and distortion energy. Distortion energy increases from cyclopropene to cyclohexene, resulting in a decrease in Diels–Alder reactivities along the series. The reactivities of different dienes are controlled by both distortion energy and interaction energy. Acyclic electron-rich 1,3-dimethoxybutadiene has stronger interaction energies than cyclopentadiene, but the extra distortion energies resulting from the *s-trans* to *s-cis* transformation and steric repulsion between terminal hydrogens of 1,3-dimethoxybutadiene in the transition states are the factors leading to higher reaction barriers. Cyclopentadiene is more reactive than 1,3-dimethoxybutadiene because it is predistorted toward transition-state geometries and requires lower distortion energies. Tetrazines undergo inverse-electron-demand Diels–Alder reactions with alkenes. The more electron-deficient 3,6-bis(trifluoromethyl)tetrazine has stronger interaction energies due to its low-lying π* orbital. In addition, 3,6-bis(trifluoromethyl)tetrazine has earlier transition states than 3,6-dimethyltetrazine, resulting in smaller distortion energies.

■ ASSOCIATED CONTENT

Ⓢ Supporting Information

Computational details and full citation of reference 19. This material is available free of charge via the Internet at http://pubs.acs.org.

■ AUTHOR INFORMATION

Corresponding Author

houk@chem.ucla.edu

Notes

The authors declare no competing financial interest.

■ ACKNOWLEDGMENTS

We are grateful to the National Science Foundation (CHE-1059084) for financial support of this research. Calculations were performed on the Hoffman2 cluster at UCLA and the Extreme Science and Engineering Discovery Environment (XSEDE), which is supported by the NSF (OCI-1053575).

■ REFERENCES

(1) Paton, R. S.; Kim, S.; Ross, A. G.; Danishefsky, S. J.; Houk, K. N. *Angew. Chem., Int. Ed.* **2011**, *50*, 10366.

(2) van Zeist, W.-J.; Bickelhaupt, F. M. *Org. Biomol. Chem.* **2010**, *8*, 3118.

(3) (a) Ess, D. H.; Houk, K. N. *J. Am. Chem. Soc.* **2007**, *129*, 10646. (b) Ess, D. H.; Houk, K. N. *J. Am. Chem. Soc.* **2008**, *130*, 10187. (c) Fernández, I.; Cossío, F. P.; Bickelhaupt, F. M. *J. Org. Chem.* **2011**, *76*, 2310. (d) Lan, Y.; Wheeler, S. E.; Houk, K. N. *J. Chem. Theory Comput.* **2011**, *7*, 2104. (e) Fernández, I.; Bickelhaupt, F. M. *J. Comput. Chem.* **2012**, *33*, 509. (f) Gordon, C. G.; Mackey, J. L.; Jewett, J. C.; Sletten, E. M.; Houk, K. N.; Bertozzi, C. R. *J. Am. Chem. Soc.* **2012**, *134*, 9199. (g) Liang, Y.; Mackey, J. L.; Lopez, S. A.; Liu, F.; Houk, K. N. *J. Am. Chem. Soc.* **2012**, *134*, 17904. (h) Fernández, I.; Bickelhaupt, F. M.; Cossío, F. P. *Chem.—Eur. J.* **2012**, *18*, 12395. (i) Lopez, S. A.; Houk, K. N. *J. Org. Chem.* **2013**, *78*, 1778. (j) Fernández, I.; Sola, M.; Bickelhaupt, F. M. *Chem.—Eur. J.* **2013**, *19*, 7416.

(4) (a) Rubin, M.; Rubina, M.; Gevorgyan, V. *Synthesis* **2006**, 1221. (b) Zhu, Z.-B.; Wei, Y.; Shi, M. *Chem. Soc. Rev.* **2011**, *40*, 5534.

(5) Wilson, M. R.; Taylor, R. E. *Angew. Chem., Int. Ed.* **2013**, *52*, 4078.

(6) (a) Patterson, D. M.; Nazarova, L. A.; Xie, B.; Kamber, D. N.; Prescher, J. A. *J. Am. Chem. Soc.* **2012**, *134*, 18638. (b) Kamber, D. N.; Nazarova, L. A.; Liang, Y.; Lopez, S. A.; Patterson, D. M.; Shih, H.-W.; Houk, K. N.; Prescher, J. A. *J. Am. Chem. Soc.* **2013**, *135*, 13680.

(7) (a) Yang, J.; Šečkute, J.; Cole, C. M.; Devaraj, N. K. *Angew. Chem., Int. Ed.* **2012**, *51*, 7476. (b) Cole, C. M.; Yang, J.; Šečkute, J.; Devaraj, N. K. *ChemBioChem* **2013**, *14*, 205. (c) Šečkute, J.; Yang, J.; Devaraj, N. K. *Nucleic Acids Res.* **2013**, *41*, e148.

(8) Yu, Z.; Pan, Y.; Wang, Z.; Wang, J.; Lin, Q. *Angew. Chem., Int. Ed.* **2012**, *51*, 10600.

(9) Wiberg, K. B.; Bartley, W. J. J *J. Am. Chem. Soc.* **1960**, *82*, 6375.

(10) Lou, Y.; Horikawa, M.; Kloster, R. A.; Hawryluk, N. A.; Corey, E. J. *J. Am. Chem. Soc.* **2004**, *126*, 8916.

(11) Cadogan, J. I. G.; Cameron, D. K.; Gosney, I.; Tinley, E. J.; Wyse, S. J.; Amaro, A. *J. Chem. Soc., Perkin Trans. 1* **1991**, 2081.

(12) Brúson, H. A.; Riener, T. W. *J. Am. Chem. Soc.* **1945**, *67*, 723.

(13) Thalhammer, F.; Wallfahrer, U.; Sauer, J. *Tetrahedron Lett.* **1990**, *31*, 6851.

(14) Wolk, J. L.; Rozental, E.; Basch, H.; Hoz, S. *J. Org. Chem.* **2006**, *71*, 3876.

(15) Roberts, J. D.; Caserio, M. C. *Basic Principles of Organic Chemistry*, 2nd ed.; W. A. Benjamin, Inc.: Menlo Park, CA, 1997.

(16) Schoenebeck, F.; Ess, D. H.; Jones, G. O.; Houk, K. N. *J. Am. Chem. Soc.* **2009**, *131*, 8121.

(17) Hayden, A. E.; Houk, K. N. *J. Am. Chem. Soc.* **2009**, *131*, 4084.

(18) The calculated activation free energies for cycloadditions of 1,3-dimethoxybutadiene **2** and Danishefsky's diene **2′** with cyclobutene are 35.2 and 35.1 kcal/mol, respectively. The transition-state structure involving **2′** is shown below.

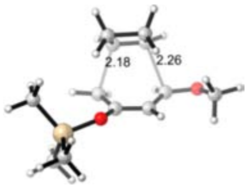

(19) Frisch, M. J., et al. *Gaussian 09*, revision C.01; Gaussian, Inc.: Wallingford, CT, 2010.

(20) Zhao, Y.; Truhlar, D. G. *Theor. Chem. Acc.* **2008**, *120*, 215.

(21) Zhao, Y.; Truhlar, D. G. *Acc. Chem. Res.* **2008**, *41*, 157.

(22) Lan, Y.; Zou, L.; Cao, Y.; Houk, K. N. *J. Phys. Chem. A* **2011**, *115*, 13906.

(23) Paton, R. S.; Mackey, J. L.; Kim, W. H.; Lee, J. H.; Danishefsky, S. J.; Houk, K. N. *J. Am. Chem. Soc.* **2010**, *132*, 9335.

(24) Zhao, Y.; Truhlar, D. G. *Phys. Chem. Chem. Phys.* **2008**, *10*, 2813.

(25) Ribeiro, R. F.; Marenich, A. V.; Cramer, C. J.; Truhlar, D. G. *J. Phys. Chem. B* **2011**, *115*, 14556.

(26) Barone, V.; Cossi, M. *J. Phys. Chem. A* **1998**, *102*, 1995.

(27) Cossi, M.; Rega, N.; Scalmani, G.; Barone, V. *J. Comput. Chem.* **2003**, *24*, 669.

(28) Glendening, E. D.; Reed, A. E.; Carpenter, J. E.; Weinhold, F. *NBO*, version 3.1; University of Wisconsin: Madison, WI, 1996.

(29) (a) Ringer, A. L.; Figgs, M. S.; Sinnokrot, M. O.; Sherrill, C. D. *J. Phys. Chem. A* **2006**, *110*, 10822. (b) Maity, S.; Sedlak, R.; Hobza, P.; Patwari, G. N. *Phys. Chem. Chem. Phys.* **2009**, *11*, 9738.

(30) (a) Politzer, P.; Abu-Awwad, F. *Theor. Chem. Acc.* **1998**, *99*, 83. (b) Kar, T.; Angyan, J. G.; Sannigrahi, A. B. *J. Phys. Chem. A* **2000**, *104*, 9953. (c) Zhang, G.; Musgrave, C. B. *J. Phys. Chem. A* **2007**, *111*, 1554.

(31) Rademacher, P. *Chem. Rev.* **2003**, *103*, 933.

(32) Staley, S. W.; Howard, A. E.; Strnad, J. T. *J. Org. Chem.* **1992**, *57*, 895.

(33) Mitchell, R. W.; Dorko, E. A.; Merritt, J. A. *J. Mol. Spectrosc.* **1968**, *26*, 197.

(34) Craig, N. C.; Borick, S. S.; Tucker, T. R.; Xiao, Y.-Z. *J. Phys. Chem.* **1991**, *95*, 3549.

(35) Villarreal, J. R.; Laane, J. *Spectrochim. Acta* **1979**, *35*, 331.

(36) Neto, N.; Di Lauro, C. *Spectrochim. Acta* **1967**, *23*, 1763.